

***In-situ* Green Synthesis of Gold Nanoparticles using Unbleached Kraft Pulp**

Nattinee Bumbudsanpharoke and Seonghyuk Ko*

Facile green synthesis of gold nanoparticles (AuNPs) on cellulose fiber was successfully achieved by reducing chloroauric acid ($\text{HAuCl}_4 \cdot 3\text{H}_2\text{O}$) by means of unbleached kraft pulp. A significant color change in pulp fiber indicating the *in-situ* formation of gold was observed with one-step synthesis in an autoclave. As-prepared AuNP-cellulose fiber nanocomposites were thoroughly characterized by UV-Vis diffuse reflectance spectroscopy (DRS), X-ray diffraction (XRD), field-emission scanning electron microscopy (FESEM), energy dispersive spectroscopy (EDS), Fourier transform infrared spectroscopy (FTIR), and X-ray photoelectron spectroscopy (XPS). Gold nanoparticles were uniformly dispersed on the surface of the fiber by the bio-reduction of Au^{3+} from metal salt to Au^0 with the α -carbonyl group and conjugated carbonyl of phenolic groups of lignin. The AuNPs formed on cellulose fibers were estimated to have average sizes of approximately 12.5, 12.4, 16.4, and 21.0 nm, depending on the concentration of Au^{3+} involved in the synthesis.

Keywords: Green synthesis; Gold nanoparticles; Unbleached kraft pulp

Contact information: Department of Packaging, Yonsei University, 1 Yonseidaegil, Wonju-si, Gangwon-do, 220-710 Korea; *Corresponding author: s.ko@yonsei.ac.kr

INTRODUCTION

Metal nanoparticles have garnered enormous attention in multidisciplinary science and engineering because of their distinctive optical, electronic, chemical, magnetic, and catalytic properties (Eustis and El-Sayed 2006; Hutchings and Edwards 2012). Gold nanoparticles (AuNPs) offer dramatically different physicochemical and catalytic properties compared to bulk gold (Kolska *et al.* 2010) and have been extensively used in various applications, including environmental catalysis (Carabineiro *et al.* 2011), energy processing (Oelhafen and Schuler 2005), chemical synthesis (Zhang *et al.* 2012), chemical and biological sensors (Saha *et al.* 2012), surface-enhanced Raman spectroscopy (SERS) (Lee *et al.* 2010), and optoelectronic applications (Mukherjee *et al.* 2012). A wide range of methods have been used to produce AuNPs with a multitude of chemical and physical processes (Haas 2013). The traditional and most widely used method for the synthesis of AuNP commonly involves the reduction of a soluble metal salt by a reducing agent or high-temperature gaseous conditions (Raveendran *et al.* 2003). Hydrazine, tri-sodium citrate, sodium borohydride, and dimethylformamide are examples of reported reducing and stabilizing agents (Pinto *et al.* 2012; Raveendran *et al.* 2003). However, exposure to these highly reactive chemicals poses potential risks to human health and the environment (He *et al.* 2009).

Thus, enormous efforts have been made to integrate green chemistry principles into metal nanoparticle synthesis to avoid accumulating an enormous quantity of toxic chemicals in the environment. Biological resources such as plant extracts, microorganisms,

biopolymers, and polysaccharides are known to be effective natural materials for alternative green synthesis of metallic nanoparticles (Iravani 2011; Hutchings and Edwards 2012). Among these ecological materials, polysaccharides are quite advantageous when utilized in green synthesis because they have an abundance of hydroxyl groups and hemiacetal reducing ends; thus, they can be used as both reducing and stabilizing agents for metal nanoparticles (Johnston and Nilsson 2012). Various polysaccharides such as buffered glucose incorporated with starch (Engelbrekt *et al.* 2009), chitosan associated with organic acid (Di Carlo *et al.* 2012), cellulose in ionic liquid (Li *et al.* 2008), guar gum (Pandey *et al.* 2013), dextran (Wang *et al.* 2010), pullulan (Choudhury *et al.* 2014), and arabinoxylan (Amin *et al.* 2013) have been employed for AuNP synthesis.

However, because gold colloids easily aggregate to yield agglomerated materials, the resulting AuNP clusters primarily serve to reduce the specific surface area, consequently reducing the sensitivity and selectivity (Azetsu *et al.* 2011; Li *et al.* 2015b). Therefore, there is intense scientific interest in the single-step integration of synthesis and immobilization of AuNPs. Azetsu *et al.* (2013) demonstrated the direct synthesis of AuNPs by TEMPO-oxidized softwood kraft paper. The aldehydic moieties in carbohydrates were reported to act as a reducing agent, while the obtained AuNPs were deposited on cellulose fibers. Johnston and Nilsson (2012) reported a mechanism of green reduction and immobilization of nanogold using lignin-containing wood fiber. They used unbleached kraft fibers and proposed that the aromatic methoxy and phenol groups of lignin play a significant role not only in reduction of gold ion (Au^{3+}) to Au^0 , but also in binding gold nanoparticles directly to the fiber surface without an external linker.

Despite the many pathways for AuNP green synthesis, there is still great interest in developing a simple and sustainable method to prepare well-defined gold nanoparticles on renewable cellulose-based fibers. To date, few studies have focused on such techniques. The present study investigated a novel, simple, one-step, “green” approach to synthesize gold nanoparticles on unbleached kraft pulp that simultaneously acts as a reducing-stabilizing agent and a substrate for AuNP immobilization. Optical, morphological, and chemical properties of the as-prepared AuNPs composited fibers were characterized using UV–Vis diffuse reflectance spectroscopy (DRS), X-ray diffraction (XRD), field-emission scanning electron microscopy (FESEM), energy dispersive spectroscopy (EDS), Fourier transform infrared spectroscopy (FTIR), and X-ray photoelectron spectroscopy (XPS). Notably, the results presented in this study offer unique insights into a facile preparative method to develop novel natural fiber composites, which can possibly be functionalized with nanomaterials to impart particular optical, catalytic, and antimicrobial properties.

EXPERIMENTAL

Materials

American Chemical Society (ACS) reagent-grade hydrogen tetrachloroaurate (III) trihydrate ($\text{HAuCl}_4 \cdot 3\text{H}_2\text{O}$; Mw. 393.83 g/mol, ACS, 99.99%) was used as received from Alfa Aesar (Ward Hill, IL, USA) without any further purification. Unbleached softwood kraft pulp was obtained in dry form from Dongil Paper (Ansan, Korea). Ultra-pure water with a specific resistivity of 18 $\text{M}\Omega \cdot \text{cm}$ was used in this study.

Synthesis of AuNP-Cellulose Fiber Nanocomposite

An aqueous solution (50.0 mM) of chloroauric acid was prepared as the nanogold precursor at room temperature. Unbleached softwood kraft pulp (UBK) was first disintegrated with a valley beater, followed by beating to an approximately 450 mL Canadian standard freeness (CSF) according to the Technical Association of the Pulp and Paper Industry (TAPPI) test methods TAPPI T200 sp-01 (2007) and TAPPI T227 om-04 (2007). After water drainage, the moisture content of the obtained pulp was approximately 83%, as determined by TAPPI T412 om-11 (2011).

Various concentrations of nanogold on UBK were prepared by adding different amounts of 50 mM chloroauric acid, as illustrated in Fig. 1. In a typical synthesis, 0.5 g of oven-dried (O.D.) pulp was suspended in 35 mL of ultra-pure water with vigorous shaking until the fibers were completely dispersed. Following preparation of the pulp suspension, a set amount of chloroauric acid solution (50 mM) was added to the pulp slurry with constant stirring and subsequently placed in an autoclave at 101.35 kPa and 121 °C for 30 min to facilitate AuNP synthesis.

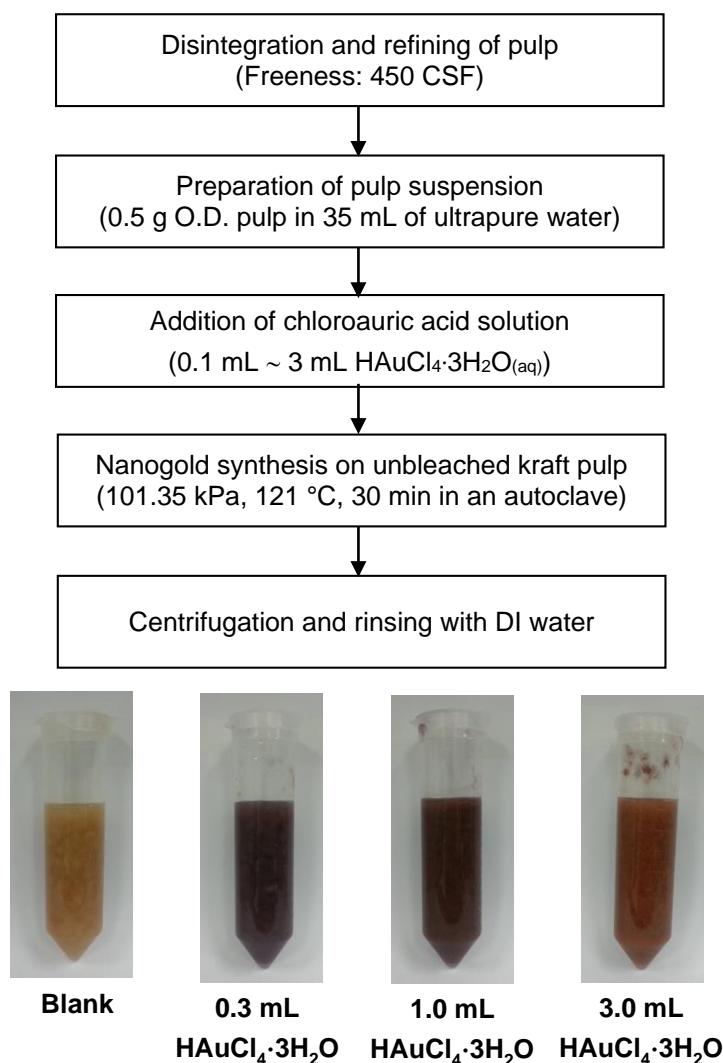


Fig. 1. Preparation of the AuNP-cellulose fiber nanocomposite

AuNP-cellulose fibers were then centrifuged and rinsed three times with ultra-pure water to remove the residual ions. Finally, diverse and colored AuNP-fiber composites were obtained and retrieved as wet pulp for further preparation of composite sheets.

The nominal Au content in the composite fibers was calculated using the weight ratio of Au³⁺ and O.D. pulp. For example, in the case of 1.0 mL of 50 mM HAuCl₄.3H₂O_(aq) dropped onto 0.5 g of O.D. pulp, HAuCl₄.3H₂O had a molarity of 5.0x10⁻⁵ mol, which amounts to 0.0197 g. Because the atomic weight of Au is 196.93 g and the molar mass of HAuCl₄.3H₂O is 393.83 g, the net amount of Au³⁺ in this slurry is calculated to be 9.85 x 10⁻³ g. Therefore, the Au³⁺ concentration of the prepared AuNP-cellulose fiber nanocomposite is 1.97 wt%. Table 1 shows the weight ratio percentage of Au³⁺ on cellulose fibers with various amounts of chloroauric acid in 0.5 g of O.D. pulp slurry.

Table 1. Nominal Ratio of Au (wt%) in Composite Fibers

Unbleached Kraft Pulp (g)	HAuCl ₄ .3H ₂ O (mL)	Au ³⁺ /cellulose (wt%)
0.5	0.1	0.20
0.5	0.2	0.39
0.5	0.3	0.59
0.5	0.5	0.98
0.5	1.0	1.97
0.5	1.2	2.36
0.5	1.5	2.95
0.5	1.7	3.35
0.5	2.0	3.94
0.5	3.0	5.91

Preparation of AuNP-Cellulose Fiber Nanocomposite Sheets

To prepare AuNP-fiber composite sheets, 2.0 g of wet AuNP-UBK pulp with approximately 90% moisture content was mixed with 300 mL of deionized (DI) water (about 0.05% consistency). The mixture was then vacuum-suctioned on a 200-mesh wire to form a wet sheet and dried in a vacuum oven at 60 °C for 8 h. Paper made of only unbleached kraft pulp, denoted blank, was also prepared for use as a reference sample. As-prepared AuNP-cellulose fiber nanocomposite sheets were named as listed in Table 1, and the calculated value of Au wt% on the basis of the relative percentage of weight ratio of chloroaurate ion (Au³⁺) against O.D. pulp weight was used in the preparation of AuNP-fibers. In addition, for the comparison of bleached fibers, 1.97 wt% of AuNP-bleached pulp composite sheet was simply prepared.

Analytical Characterization

UV-Vis diffuse reflectance spectra of as-prepared AuNP-cellulose fiber sheets were acquired using a double-beam V-600 spectrophotometer (Jasco, Japan) with an attached integrating sphere in the wavelength range of 200 to 800 nm. X-ray diffraction patterns were obtained on an X-ray diffractometer (D2 Phaser, Bruker, Germany) with Ni-filtered CuK α radiation ($\lambda=1.5406$ Å). The surface morphology of the composite sheet was observed with a field-emission scanning electron microscope (FE-SEM Quanta FEG 250, FEI, USA) in backscattered electron (BE) mode after sputtering platinum/palladium onto the specimen using a Cressington Sputter Coater 108 auto (Cressington Scientific Instruments, Watford, UK). Further elemental analysis was carried out with an energy-dispersive X-ray spectrometer (EDS, Bruker AXS, Japan) attached to the FESEM. FTIR

analyses were performed using a Spectrum 65 FTIR (Perkin Elmer, USA). Each spectrum was collected in attenuated total reflectance (ATR) mode with 16 scans and 2 cm^{-1} resolution in the range of 4000 to 400 cm^{-1} . The surface chemical compositions of both blank and AuNP-cellulose fiber nanocomposites were analyzed with X-ray photoelectron spectroscopy (XPS K-alpha, Thermo VG, UK) with a monochromated Al X-ray source ($h\nu = 1486.6\text{ eV}$).

RESULTS AND DISCUSSION

Characterization of AuNP-Cellulose Fiber Nanocomposites

This study established a simple green reduction method to prepare AuNP-cellulose fiber nanocomposites using unbleached kraft pulp. As described in detail in the experimental section, upon the addition of 50 mM chloroauric acid to a pulp slurry, the color of the pulp gradually changed to a darker shade after a 30-min incubation in an autoclave. Figure 2 represents the apparent color change of AuNP-cellulose fiber nanocomposites as a function of the weight ratio of Au^{3+} . The color went through a series of changes from pale yellow (blank), gray ($0.20\text{ wt}\%$), purple ($0.98\text{ wt}\%$), and wine-red ($2.36\text{ wt}\%$) to dark wine-red brown ($5.91\text{ wt}\%$). This diverse color spectrum is attributed to the surface plasmon resonance (SPR) of AuNPs (Kumari and Philip 2013), implying the direct synthesis of nanogold on the fiber surface. It is generally known that the SPR effect is a result of the resonance interaction of incoming visible electromagnetic radiation with collective plasmon oscillations on the metal surface (Johnston and Lucas 2011).

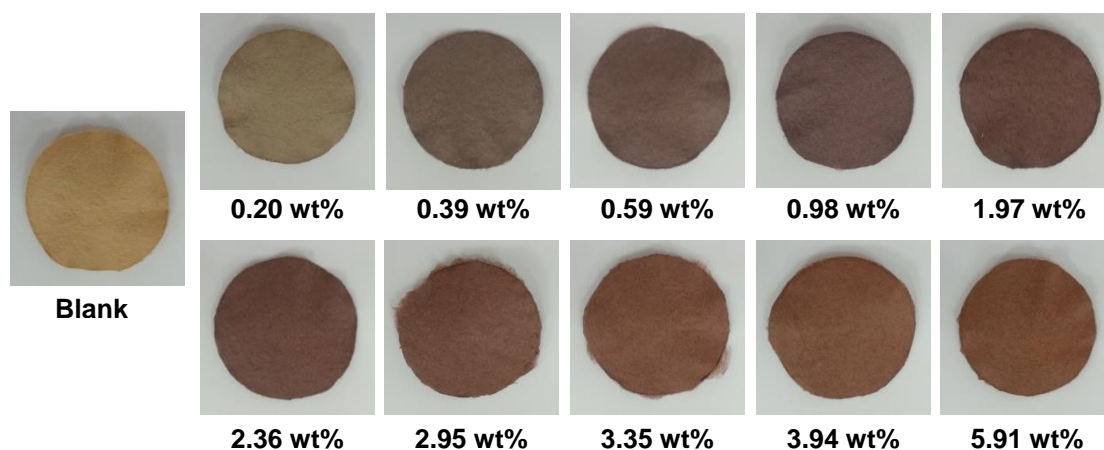


Fig. 2. AuNP-cellulose fiber nanocomposite sheets prepared with various concentrations of Au(III)

To verify the formation of AuNPs on cellulose fiber, the blank sample (pulp fibers only), and AuNP-cellulose fiber nanocomposites were characterized using UV-Vis spectroscopy because AuNPs are known to show a plasmon resonance band in the region of 530 to 550 nm (Agnihotri *et al.* 2009; Kumari and Philip 2013). Figure 3 presents the UV-Vis diffuse reflectance spectra of composite samples. The blank sample presents only the multiple peaks in the region of 200 to 300 nm , which can be assigned to hexenuronic acid and aromatic lignin (Boonstra and Tjeerdsma 2006; Lähdetie *et al.* 2009). In contrast,

AuNP-cellulose fiber composite samples exhibit an additional absorption peak in the region of 530 to 540 nm that can be attributed to the SPR band of AuNPs. The intensity of the absorption band gradually increased with increasing concentration of Au³⁺, and the peak broadened at a relatively higher concentration of Au³⁺. These results suggest that the AuNPs are highly dispersed on the cellulose fiber, and this increase in metal nanoparticle dispersion results in increased interaction among AuNPs, leading to broadening of the SPR. A similar result was observed by Pulit and Banach (2014) in the preparation of AuNPs using *Dog Rose* aqueous extract as a reducing agent. They found that the higher concentrations of gold ions involved in the synthesis resulted in lower and broader UV-Vis absorption spectra of AuNPs because of the formation of larger particles as well as a polymodal size distribution. In addition, as can be seen in Fig. 3, the absorption peak of AuNPs in bleached kraft pulp composite is not discernable compared to that of unbleached kraft pulp nanocomposite. This indicates the Au nanoparticles were not effectively produced, due to the lack of a chemical group that was susceptible to being oxidized. Johnston and Nilsson (2012) have reported that cellulose shows lower effectiveness in forming and bonding AuNPs than UBK, which has abundant reducing ends from phenolic and methoxy groups attached to the electron-rich aromatic rings from lignin.

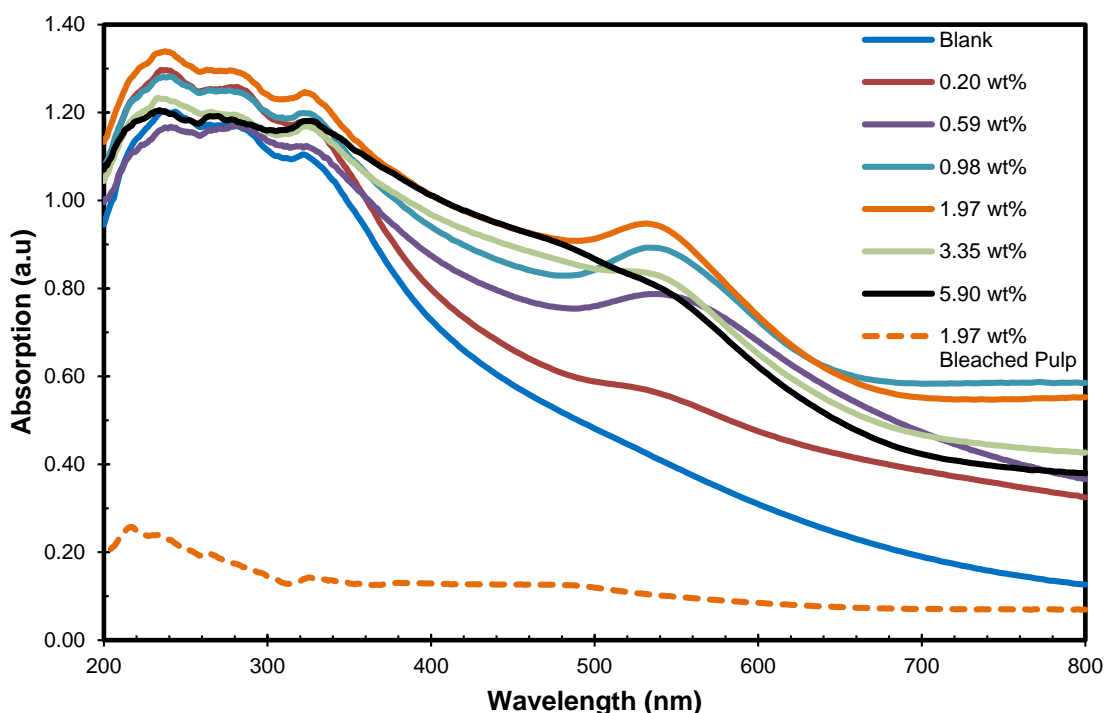


Fig. 3. UV/Vis diffuse reflectance spectra of AuNP-cellulose fiber nanocomposite sheets

XRD was used for further characterization of the crystallographic structure and AuNP grain size. The XRD patterns of blank and AuNP-cellulose fiber composites are shown in Fig. 4. The dominant peak at a 2-theta near 23.1° was observed for all samples; this originates from the parallel chain structure of cellulose crystalline (002) (Dinand *et al.* 2002; Zhao *et al.* 2007). In addition, AuNP-fiber composite sheets showed four Bragg reflection peaks at 2-theta values of nearly 38.6°, 44.9°, 65.0°, and 78.0°, which are indexed to the (111), (200), (220), and (311) planes of the face-centered cubic (fcc) lattice of gold

(JCPDS no. 04-0784), respectively (Sen *et al.* 2013). The XRD results indicate that the pure metallic gold crystals were effectively formed on cellulose fiber.

Average gold particle sizes in AuNP-cellulose fiber nanocomposites were estimated based on the Scherrer equation from the full width at half maximum (FWHM) intensity as,

$$D = \frac{K\lambda}{b \cdot \cos\theta} \quad (1)$$

where D is the grain size, K is the Scherrer constant value (0.9 to 1), λ is the wavelength of the X-ray radiation, b is the FWHM, and θ is the Bragg angle (Aromal and Philip 2012). Using this formula, the average size of AuNPs was calculated to be 12.5, 12.4, 16.4, and 21.0 nm in order of increasing concentration of chloroauric acid, *i.e.*, 0.59, 0.98, 1.97, and 5.90 wt%, respectively. This difference in grain size influences the color of the AuNP-cellulose fiber nanocomposites, as shown in Fig. 2. A similar result was reported by Johnston and Lucas (2011), wherein the differences in particle size of the AuNP imparted various colors to AuNP-wool fiber.

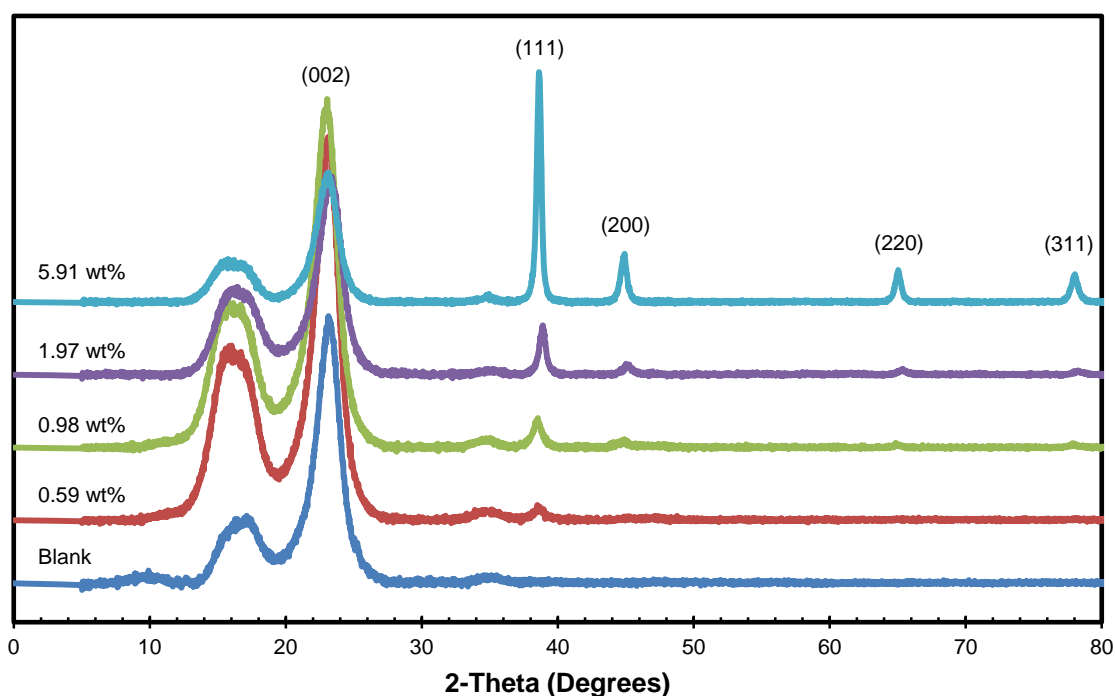


Fig. 4. XRD patterns of blank and AuNP-cellulose fiber nanocomposite sheets

The formation and deposition of gold particles on the surface of cellulose fiber were clearly revealed by FESEM in BE mode. Images are shown in Fig. 5, along with representative EDS elemental spectra. In Figs. 5(b-d), AuNPs can be readily identified as white dots dispersed over the surface compared to the smooth and clean surface of cellulose fiber (Fig. 5(a)). These images confirm that AuNPs were uniformly formed on the surface of fibers and distinctly indicate that more chloroaurate ions (Au^{3+}) involved in the preparation led to increases in the number and coverage of AuNPs on cellulose fibers. This result is consistent with the gradual broadening of SPR spectra and sharpness in diffraction

peaks, as shown in Figs. 3 and 4. Similar results were observed by Ngo *et al.* (2012): the population of AuNPs on cellulose fiber increased linearly with the concentration of AuNP precursor solution.

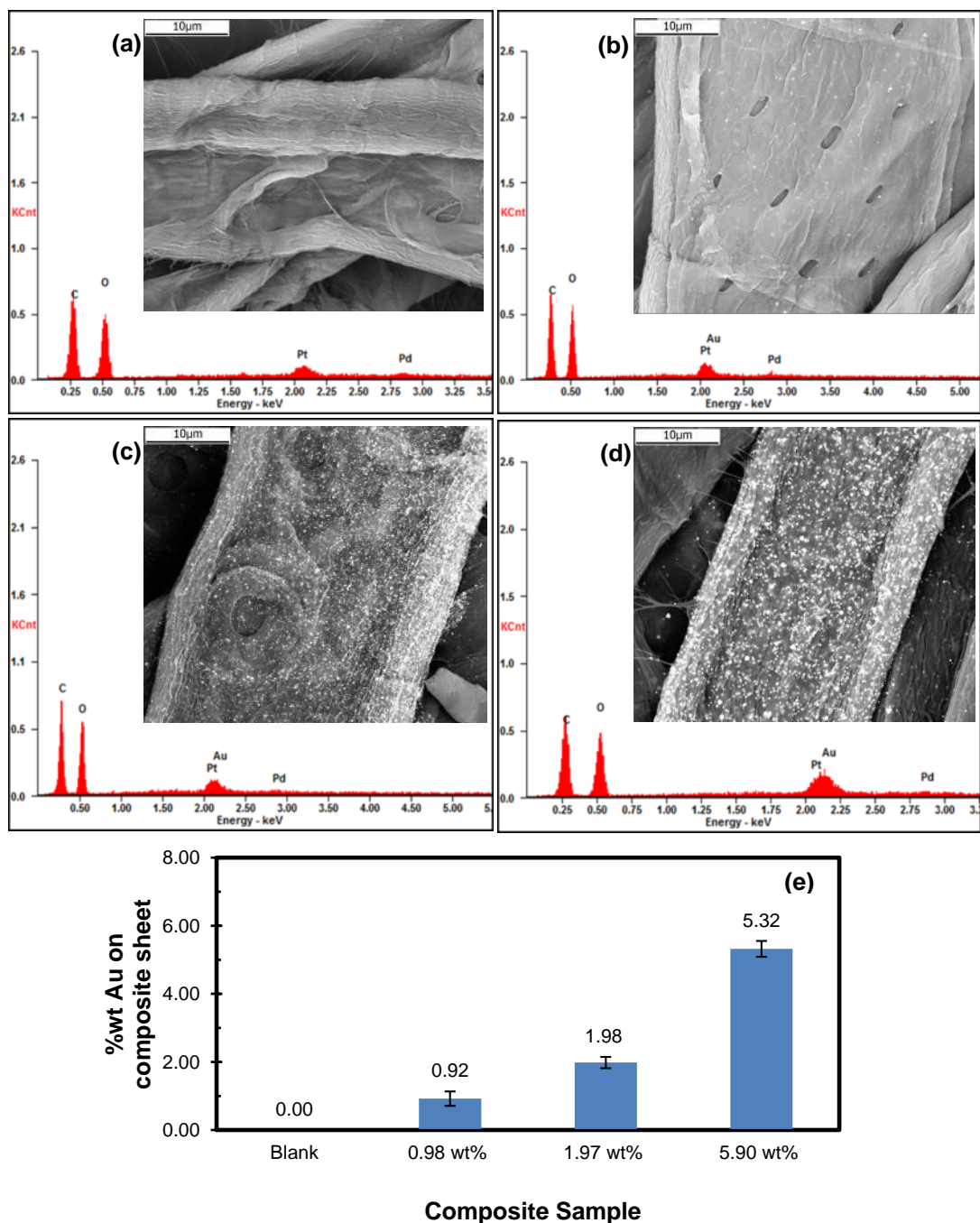


Fig. 5. Backscattered electron FESEM images at 3,000x magnification and corresponding EDS spectra of (a) blank and AuNP-fiber composites of (b) 0.98 wt%, (c) 1.97 wt%, and (d) 5.90 wt%; (e) EDS analysis of the Au component

Figure 5(e) presents the average content of Au obtained by EDS microanalysis. The average was determined from five different areas on the blank and AuNP-cellulose fiber nanocomposites. The results are consistent with the proposed weight percent of Au³⁺

precursor and tended to increase in proportion to the concentration of Au^{3+} , implying that the gold ions were effectively reduced to AuNPs.

Figure 6 shows the FTIR spectra of the blank and AuNP-cellulose fiber nanocomposites. No distinguishing peaks were observed when comparing the blank and AuNP composite sheets, with the exception of one visible peak integrated over the range 1550 to 1650 cm^{-1} , which is assigned to the aromatic vibration of lignin, conjugated C=O stretching of the phenolic group, and C-O stretching from lignin (Popescu *et al.* 2010; Wang *et al.* 2009). In particular, as shown in Fig. 6(b), the intensity of the peak at 1580 to 1585 cm^{-1} , which is associated with the α -carbonyl group on lignin (Bykov 2008), was reduced with higher Au^{3+} concentration. This is compatible with the clustering and movement of Au^0 species resulting from Au^{3+} bio-reduction occurring in the electron-rich lignin component and is indicative of participation of the lignin component in AuNP synthesis.

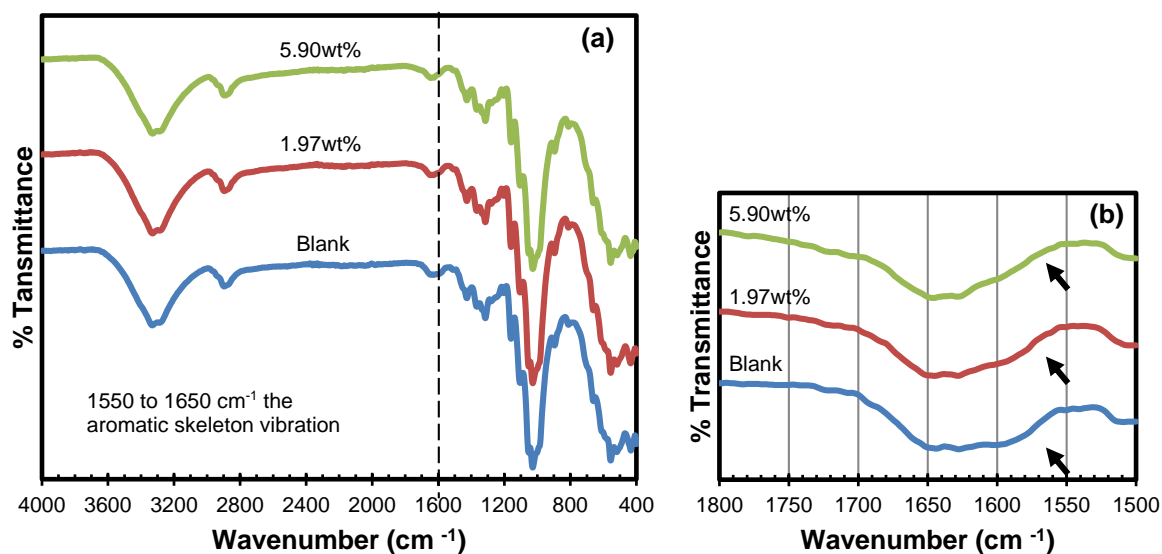


Fig. 6. (a) FTIR spectra of blank and AuNP–cellulose fiber nanocomposites; (b) the spectra at wavenumbers 1500 to 1800 cm^{-1}

Previous studies have reported similar mechanisms of nanometal synthesis. Tagad *et al.* (2014) demonstrated that the aldehyde groups and hemiacetal reducing ends of polysaccharides facilitate the reduction of Au^{3+} to Au^0 . Li *et al.* (2015a) observed that the vibration peak of C=O from cellulose fibers slightly decreased with higher concentration of silver ions. Kan *et al.* (2005) proposed that metal ions attract electrons from carbonyl to form metal crystal nuclei and subsequently grow into metal particles. Thus, it is believed that the conjugated carbonyl groups in lignin play a significant role in the reduction of gold ions into metallic gold, as depicted in Fig. 7.

Figure 8 displays the XPS survey scan spectra of blank and AuNP-fiber composite sheets. As seen in Fig. 8(a), both samples exhibited C1s and O1s core level spectra that can be attributed to the carbon and oxygen present in the cellulose fiber (Johansson 2002). An additional peak corresponding to gold appeared at a binding energy of 83 to 88 eV in the gold composite sheet. Figure 8(b) shows the XPS spectrum of the Au4f region of the AuNP-fiber composite. Doublet peaks were observed at BE positions of 84.08 and 87.78 eV, assigned to the $\text{Au}4f_{7/2}$ and $\text{Au}4f_{5/2}$ core levels of metallic gold (Au^0), respectively

(Vitale *et al.* 2011; Zhao *et al.* 2006). This result is in accordance with the XRD characterization and provides further evidence that gold ions (Au^{3+}) were successfully reduced to metallic pure Au bound to the cellulose fibers.

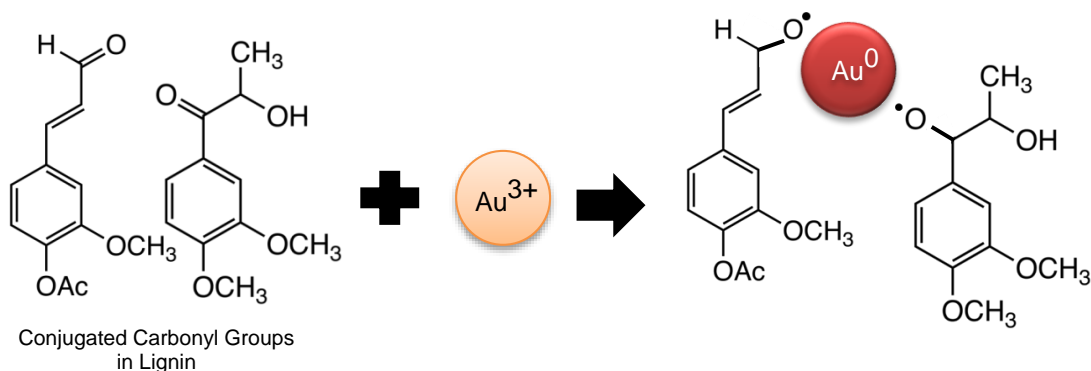


Fig. 7. Schematic of a reaction mechanism for AuNP synthesis on the conjugated carbonyl groups of lignin

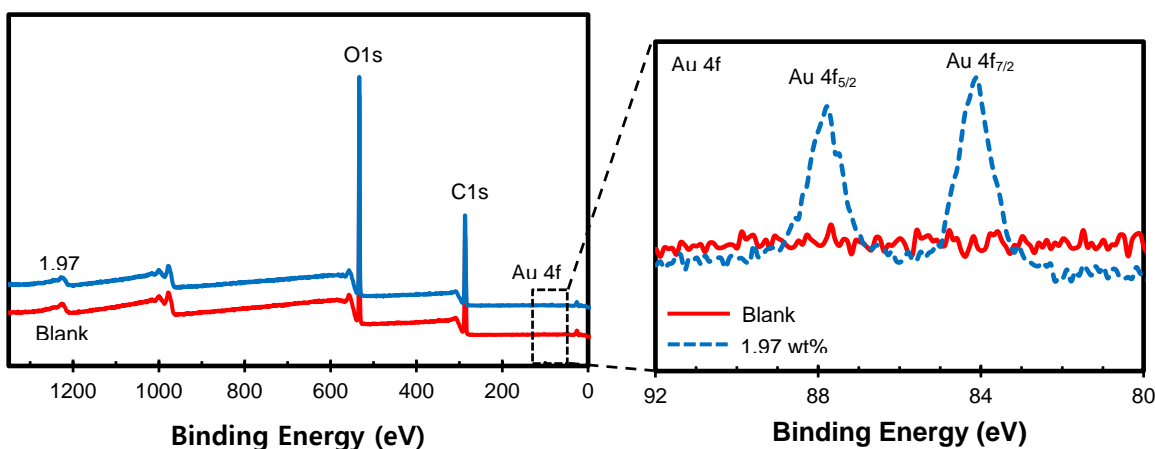


Fig. 8. (a) XPS survey scan spectra and (b) the Au4f region spectra of blank and AuNP-cellulose fiber nanocomposite sheets

CONCLUSIONS

1. AuNP-cellulose fiber nanocomposites were successfully prepared through a facile green method. The resulting purple-colored fiber composite showed a typical UV-Vis absorbance spectra at approximately 530 nm, which is attributed to SPR of AuNPs.
2. FESEM images clearly revealed that AuNPs were formed and distributed over the surface of the fiber and were identified as metallic gold (Au^0) by an XPS narrow scan of the Au4f region.
3. It was also found that the α -carbonyl group on lignin decreased with AuNP synthesis, suggesting that lignin plays an important role in efficient bio-reduction of gold ions into metallic gold and binding to the fiber surface.

4. The preparation procedure presented here provides a simple and sustainable route to synthesize and immobilize AuNPs in an environmentally friendly manner. The comparative study of AuNP synthesis on cellulose fiber with a different synthetic condition such as reflux system under normal pressure is a topic for future work.

REFERENCES CITED

- Agnihotri, M., Joshi, S., Kumar, A. R., Zinjarde, S., and Kulkarni, S. (2009). "Biosynthesis of gold nanoparticles by the tropical marine yeast *Yarrowia lipolytica* NCIM 3589," *Mater. Lett.* 63(15), 1231-1234. DOI: 10.1016/j.matlet.2009.02.042
- Amin, M., Iram, F., Iqbal, M. S., Saeed, M. Z., Raza, M., and Alam, S. (2013). "Arabinoxylan-mediated synthesis of gold and silver nanoparticles having exceptional high stability," *Carbohydr. Polym.* 92(2), 1896-900. DOI: 10.1016/j.carbpol.2012.11.056
- Aromal, S. A., and Philip, D. (2012). "Benincasa hispida seed mediated green synthesis of gold nanoparticles and its optical nonlinearity," *Physica E* 44(7), 1329-1334. DOI: 10.1016/j.physe.2012.02.013
- Azetsu, A., Koga, H., Isogai, A., and Kitaoka, T. (2011). "Synthesis and catalytic features of hybrid metal nanoparticles supported on cellulose nanofibers," *Catalysts* 1(1), 83-96. DOI: 10.3390/Catal1010083
- Azetsu, A., Koga, H., Yuan, L. Y., and Kitaoka, T. (2013). "Direct synthesis of gold nanocatalysts on tempo-oxidized pulp paper containing aldehyde groups," *BioResources* 8(3), 3706-3717. DOI: 10.15376/biores.8.3.3706-3717
- Boonstra, M. J., and Tjeerdsma, B. (2006). "Chemical analysis of heat treated softwoods," *Holz Roh Werkst.* 64(3), 204-211. DOI: 10.1007/s00107-005-0078-4
- Bykov, I. (2008). "Characterization of natural and technical lignins using FTIR spectroscopy," Luleå University of Technology, Luleå, Sweden
- Carabineiro, S. A. C., Bogdanchikova, N., Avalos-Borja, M., Pestryakov, A., Tavares, P. B., and Figueiredo, J. L. (2011). "Gold supported on metal oxides for carbon monoxide oxidation," *NanoRes.* 4(2), 180-193. DOI: 10.1007/s12274-010-0068-7
- Choudhury, A. R., Malhotra, A., Bhattacharjee, P., and Prasad, G. S. (2014). "Facile and rapid thermo-regulated biomineralization of gold by pullulan and study of its thermodynamic parameters," *Carbohydr. Polym.* 106(1), 154-159. DOI: 10.1016/j.carbpol.2014.01.072
- Di Carlo, G., Curulli, A., Toro, R. G., Bianchini, C., De Caro, T., Padeletti, G., Zane, D., and Ingo, G. M. (2012). "Green synthesis of gold-chitosan nanocomposites for caffeic acid sensing," *Langmuir* 28(12), 5471-5479. DOI: 10.1021/la204924d
- Dinand, E., Vignon, M., Chanzy, H., and Heux, L. (2002). "Mercerization of primary wall cellulose and its implication for the conversion of cellulose I→ cellulose II," *Cellulose* 9(1), 7-18. DOI: 10.1023/A:1015877021688
- Engelbrekt, C., Sørensen, K. H., Zhang, J., Welinder, A. C., Jensen, P. S., and Ulstrup, J. (2009). "Green synthesis of gold nanoparticles with starch–glucose and application in bioelectrochemistry," *J. Mater. Chem.* 19(42), 7839-7847. DOI: 10.1039/b911111e
- Eustis, S., and El-Sayed, M. A. (2006). "Why gold nanoparticles are more precious than pretty gold: Noble metal surface plasmon resonance and its enhancement of the radiative and nonradiative properties of nanocrystals of different shapes," *Chem. Soc. Rev.* 35(3), 209-217. DOI: 10.1039/B514191e

- Haas, K. H. (2013). "Industrial relevant production processes for nanomaterials and nanostructures," in: *Safety aspects of engineered nanomaterials*, W. Luther and A. Zweck (eds). CRC Press, Boca Raton, FL, 29-62. DOI: 10.1201/b15261-3
- He, F., Liu, J., Roberts, C. B., and Zhao, D. (2009). "One-step "green" synthesis of Pd nanoparticles of controlled size and their catalytic activity for trichloroethene hydrodechlorination," *Ind. Eng. Chem. Res.* 48(14), 6550-6557. DOI: 10.1021/ie801962f
- Hutchings, G. J., and Edwards, J. K. (2012). "Application of gold nanoparticles in catalysis," in: *Metal Nanoparticles and Nanoalloys*, R. L. Johnston and J. P. Wilcoxon (eds). Elsevier Ltd, Oxford, UK, 249-293. DOI: 10.1016/B978-0-08-096357-0.00006-6
- Iravani, S. (2011). "Green synthesis of metal nanoparticles using plants," *Green Chem.* 13(10), 2638-2650. DOI: 10.1039/C1gc15386b
- Johansson, L. S. (2002). "Monitoring fibre surfaces with XPS in papermaking processes," *Mikrochim. Acta* 138(3-4), 217-223. DOI: 10.1007/s006040200025
- Johnston, J. H., and Lucas, K. A. (2011). "Nanogold synthesis in wool fibres: novel colourants," *Gold Bull.* 44(2), 85-89. DOI: 10.1007/s13404-011-0012-y
- Johnston, J. H., and Nilsson, T. (2012). "Nanogold and nanosilver composites with lignin-containing cellulose fibres," *J. Mater. Sci.* 47(3), 1103-1112. DOI: 10.1007/s10853-011-5882-0
- Kan, C. X., Cai, W. P., Li, C. C., and Zhang, L. D. (2005). "Optical studies of polyvinylpyrrolidone reduction effect on free and complex metal ions," *J. Mater. Res.* 20(2), 320-324. DOI: 10.1557/Jmr.2005.0039
- Kolska, Z., Riha, J., Hnatowicz, V., and Svorcik, V. (2010). "Lattice parameter and expected density of Au nano-structures sputtered on glass," *Mater. Lett.* 64(10), 1160-1162. DOI: 10.1016/j.matlet.2010.02.038
- Kumari, M. M., and Philip, D. (2013). "Facile one-pot synthesis of gold and silver nanocatalysts using edible coconut oil," *Spectrochim. Acta A* 111, 154-160. DOI: 10.1016/j.saa.2013.03.076
- Lähdetie, A., Liitiä, T., Tamminen, T., and Jääskeläinen, A.-S. (2009). "Reflectance UV-Vis and UV resonance Raman spectroscopy in characterization of kraft pulps," *BioRes.* 4(4), 1600-1619.
- Lee, C. H., Tian, L., and Singamaneni, S. (2010). "Paper-based SERS swab for rapid trace detection on real-world surfaces," *ACS Appl. Mater. Inter.* 2(12), 3429-3435. DOI: 10.1021/am1009875
- Li, R., He, M., Li, T., and Zhang, L. (2015a). "Preparation and properties of cellulose/silver nanocomposite fibers," *Carbohydr. Polym.* 115, 269-275. DOI: 10.1016/j.carbpol.2014.08.046
- Li, Y., Liu, Y., Liu, J., Liu, J., Tang, H., Cao, C., Zhao, D., and Ding, Y. (2015b). "Molecularly imprinted polymer decorated nanoporous gold for highly selective and sensitive electrochemical sensors," *Sci. Rep.* 5, 7699(1-8). DOI: 10.1038/srep07699
- Li, Z., Friedrich, A., and Taubert, A. (2008). "Gold microcrystal synthesis via reduction of HAuCl₄ by cellulose in the ionic liquid 1-butyl-3-methyl imidazolium chloride," *J. Mater. Chem.* 18(9), 1008-1014. DOI: 10.1039/B716135M
- Mukherjee, P., Nandi, S., and Nandi, A. K. (2012). "Optoelectronic properties of RNA-polyaniline-dendritic gold nanobiocomposite," *Synth. Met.* 162(11), 904-911. DOI: 10.1016/j.synthmet.2012.04.004

- Ngo, Y. H., Li, D., Simon, G. P., and Garnier, G. (2012). "Gold nanoparticle–paper as a three-dimensional surface enhanced raman scattering substrate," *Langmuir* 28(23), 8782-8790. DOI: 10.1021/la3012734 |
- Oelhafen, P., and Schuler, A. (2005). "Nanostructured materials for solar energy conversion," *Solar Energy* 79(2), 110-121. DOI: 10.1016/j.solener.2004.11.004
- Pandey, S., Goswami, G. K., and Nanda, K. K. (2013). "Green synthesis of polysaccharide/gold nanoparticle nanocomposite: An efficient ammonia sensor," *Carbohydr. Polym.* 94(1), 229-234. DOI: 10.1016/j.carbpol.2013.01.009
- Pinto, R. J., Neves, M. C., Neto, C. P., and Trindade, T. (2012). "Composites of cellulose and metal nanoparticles," in: *Nanocomposites–New Trends and Developments*, F. Ebrahimi (eds). InTech, Croatia, 73-96. DOI: 10.5772/3389
- Popescu, C. M., Popescu, M. C., and Vasile, C. (2010). "Characterization of fungal degraded lime wood by FT-IR and 2D IR correlation spectroscopy,," *Microchem. J.* 95(2), 377-387. DOI: 10.1016/j.microc.2010.02.021
- Pulit, J., and Banach, M. (2014). "Preparation of nanosilver and nanogold based on *Dog Rose* aqueous extract," *Bioinorg. Chem. Appl.* 2014(1), 1-14 (Article ID 658935). DOI: 10.1155/2014/658935
- Raveendran, P., Fu, J., and Wallen, S. L. (2003). "Completely "green" synthesis and stabilization of metal nanoparticles," *J. Am. Chem. Soc.* 125(46), 13940-13941. DOI: 10.1021/ja029267j
- Saha, K., Agasti, S. S., Kim, C., Li, X., and Rotello, V. M. (2012). "Gold nanoparticles in chemical and biological sensing," *Chem. Rev.* 112(5), 2739-2779. DOI: 10.1021/cr2001178
- Sen, I. K., Maity, K., and Islam, S. S. (2013). "Green synthesis of gold nanoparticles using a glucan of an edible mushroom and study of catalytic activity," *Carbohydr. Polym.* 91(2), 518-528. DOI: 10.1016/j.carbpol.2012.08.058
- Tagad, C. K., Rajdeo, K. S., Kulkarni, A., More, P., Aiyer, R. C., and Sabharwal, S. (2014). "Green synthesis of polysaccharide stabilized gold nanoparticles: chemo catalytic and room temperature operable vapor sensing application," *RSC Adv.* 4(46), 24014-24019. DOI: 10.1039/C4ra02972k
- TAPPI T200 sp-01. (2007). "Laboratory beating of pulp (Valley beater method)," TAPPI Press, Atlanta, GA.
- TAPPI T227 om-04. (2007). "Freeness of Pulp (Canadian Standard Method)," TAPPI Press, Atlanta, GA.
- TAPPI T412 om-11. (2011). "Moisture in pulp, paper and paperboard," TAPPI Press, Atlanta, GA.
- Vitale, F., Fratoddi, I., Battocchio, C., Piscopiello, E., Tapfer, L., Russo, M. V., Polzonetti, G., and Giannini, C. (2011). "Mono- and bi-functional arenethiols as surfactants for gold nanoparticles: synthesis and characterization," *Nanoscale Res. Lett.* 6, 103. DOI: 10.1186/1556-276x-6-103
- Wang, H., Huang, L., and Lu, Y. (2009). "Preparation and characterization of micro- and nano-fibrils from jute," *Fiber. Polym.* 10(4), 442-445. DOI: 10.1007/s12221-009-0442-9
- Wang, Y., Zhan, L., and Huang, C. Z. (2010). "One-pot preparation of dextran-capped gold nanoparticles at room temperature and colorimetric detection of dihydralazine sulfate in uric samples," *Analytical Methods* 2(12), 1982-1988. DOI: 10.1039/C0ay00470g

- Zhang, Y., Cui, X., Shi, F., and Deng, Y. (2012). "Nano-gold catalysis in fine chemical synthesis," *Chem. Rev.* 112(4), 2467-505. DOI: 10.1021/cr200260m
- Zhao, W., Xu, J. J., Shi, C. G., and Chen, H. Y. (2006). "Fabrication, characterization and application of gold nano-structured film," *Electrochem. Commun.* 8(5), 773-778. DOI: 10.1016/j.elecom.2006.03.009
- Zhao, H. B., Kwak, J. H., Zhang, Z. C., Brown, H. M., Arey, B. W., and Holladay, J. E. (2007). "Studying cellulose fiber structure by SEM, XRD, NMR and acid hydrolysis," *Carbohydr. Polym.* 68(2), 235-241. DOI: 10.1016/j.carbpol.2006.12.013

Article submitted: March 24, 2015; Peer review completed: July 20, 2015; Revised version received: July 29, 2015; Accepted: July 30, 2015; Published: August 10, 2015. DOI: 10.15376/biores.10.4.6428-6441